

# ION OPTICAL STRAY FIELD ANALYSIS OF AN ESR DIPOLE

B. Schillinger, T. Weiland, Darmstadt University of Technology, Germany  
B. Langenbeck, GSI, Germany

## Abstract

The ion optical characteristics of the injection into the ESR are calculated up to second order. The three dimensional model of an ESR dipole magnet forms the basis of our computations. Special efforts have been spent on an accurate approximation of the lateral stray field over a distance of 2m, in which the ion beam enters the ESR dipole tangentially. The reference trajectory and the first and second order transformation coefficients are calculated solving the corresponding differential equations numerically. For this purpose we have developed a new ion optics section as part of the MAFIA postprocessing module P. The differential equations are set up and solved automatically using the simulated magnetic field distribution. The new implemented section is general and allows the easy calculation of beam trajectories and optical characteristics corresponding to arbitrary numerically calculated magnetic fields. As special feature also phase space monitors along a curved reference trajectory can be defined. We will give a short introduction into the method and discuss the results in case of the ESR injection.

## 1 INTRODUCTION

The location of the Experimental Storage Ring (ESR) [1] in the whole GSI accelerator complex requires an unusual beam guide for the injection. Between the inflector and the in-ring septum magnet the ion beam has to pass the lateral fringe field of a dipole magnet over a distance of two meters (figure 1). To get a better knowledge about the influence of this perturbation on the beam ellipse we have made a 3D simulation of one quarter of the whole dipole magnet. Further, we have used this simulation results as basis for numerical calculations of the curved injection line and the ion optical transfer map up to second order.

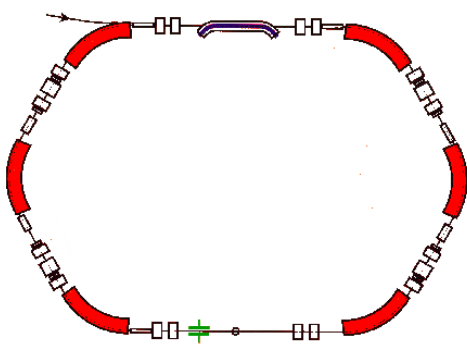


Figure 1: Layout of the ESR with injection line.

## 2 DIPOLE DIMENSIONS AND SIMULATION PARAMETERS

The bending system of the ESR consists of six  $60^\circ$  sector magnets with a maximum field strength of 1.6 T. In the following we choose a working point of 1 T. In this case the effective bending radius is 6.324 m in respect of an effective field boundary of 4 cm at the magnet ends [2].

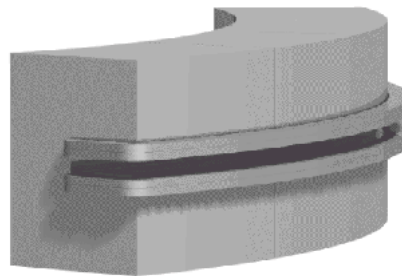


Figure 2: 3D view of an ESR Dipole magnet.

The magnet has a non-orthogonal exit face (exit angle  $7.5^\circ$ ), which leads to difficulties in view of the mesh generation. Therefore we use a coupled coordinate system [3] as indicated in figure 3. Further, we take advantage of the two symmetry planes and decided to shorten the simulated sector up to  $17^\circ$  in order to reduce the number of mesh points.

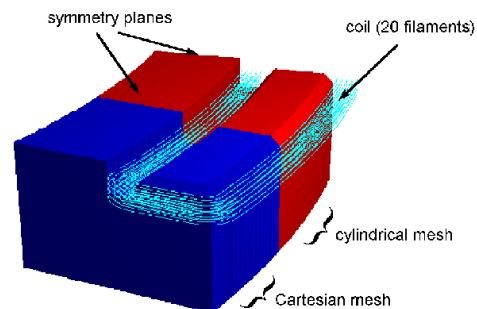


Figure 3: Approximated part of the dipole which is used for the field calculation.

## 3 OPTICS OF THE INJECTION

Being interested in the optics of the injection, we introduce a local coordinate system  $x, y, z$  along the injection line as shown in figure 4. The fixed global coordinate system  $\xi, \psi, \zeta$  is placed at the intersection point of central tra-

jectory and exit face,  $\zeta$  points in normal direction of the dipole's mid plane.

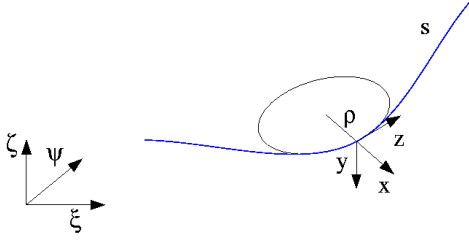


Figure 4: Global and local coordinate system.

In matrix notation the whole injection line can be subdivided in three parts: a drift space  $M_0$  from the inflector magnet to the dipole, the stray field region of the dipole  $M_s$  and a drift space up to the septum magnet in the ring  $M_1$ . The combined map  $\mathbf{x}^1 = M_1 M_s M_0 \mathbf{x}^0$  describes the optical transformation of an initial phase space vector  $\mathbf{x}^0 = (x, x', y, y', l, \delta)^0$  located at the inflector magnet to a final vector  $\mathbf{x}^1 = (x, x', y, y', l, \delta)^1$  located at the in-ring septum magnet.

Up to second order the combined map takes the expansion

$$x_i^1 = \sum_{j=1}^6 (x_i^1 | x_j^0) x_j^0 + \sum_{j,k=1}^6 (x_i^1 | x_j^0 x_k^0) x_j^0 x_k^0, i = 1, \dots, 6.$$

The first order coefficients  $C_x = (x_1^1 | x_2^0)$ ,  $S_x = (x_1^1 | x_2^0)$ ,  $C_y = (x_3^1 | x_3^0)$  and  $S_y = (x_3^1 | x_4^0)$ , the so called principal trajectories, are solutions of the homogeneous differential equations

$$\begin{aligned} C_x''(s) + k_x(s)C_x(s) &= 0, & C_y''(s) + k_y(s)C_y(s) &= 0, \\ S_x''(s) + k_x(s)S_x(s) &= 0, & S_y''(s) + k_y(s)S_y(s) &= 0, \end{aligned}$$

with boundary conditions  $C(0) = 1$ ,  $C'(0) = 0$ ,  $S(0) = 0$ ,  $S'(0) = 1$ . The prime denotes derivation with respect to the path length  $s$ . The stiffness parameter functions  $k_x(s)$  and  $k_y(s)$  depend on the field expansion coefficients

$$\begin{aligned} h(s) &= \left. \frac{q}{p_0} B_y(s) \right|_{x=y=0} \\ k(s) &= \left. \frac{q}{p_0} \frac{\partial B_y(s)}{\partial x} \right|_{x=y=0} \end{aligned}$$

and are given by  $k_y(s) = -k(s)$  and  $k_x(s) = h^2(s) + k(s)$ .

The first order dispersion  $D_x = (x_1^1 | x_6^0)$  and the second order coefficients  $q_{ijk} = (x_i^1 | x_j^0 x_k^0)$  are solutions of the inhomogeneous differential equations

$$q_{ijk}''(s) + k_x(s)q_{ijk}(s) = f_{ijk}(s),$$

resp.

$$q_{ijk}''(s) + k_y(s)q_{ijk}(s) = f_{ijk}(s)$$

with boundary conditions  $q_{ijk}(0) = 0$ ,  $q'_{ijk}(0) = 0$  and varying driving functions  $f_{ijk}(s)$ . The driving functions

depend on second order field derivatives in normal ( $x$ ) and tangential ( $z$ ) direction and are listed in [4, 5].

In our case the stiffness parameters and driving functions are non-constant and not analytically given. Therefore we will simultaneously integrate the reference trajectory, evaluate the stiffness parameters and driving functions and solve the introduced differential equations on the basis of the simulated field data. To assure the accuracy of the solution, we tested the procedure on an idealized dipole magnet with parallel ends[6].

## 4 SIMULATION RESULTS

### 4.1 Field Calculations

We have performed a nonlinear calculation of an ESR dipole magnet with the parameters introduced in section 2 using the static solver S of the MAFIA package[7], which has been modified to solve the field equations in a coupled coordinate system. Figure 5 shows the simulation results for the Field in the mid plane at an azimuthal cut compared with measurements. The two curves fit very well, the deviations are lower than 0.1%, which means that the simulated lateral fringe field can be used for further ion optical treatments. An additional reduction of the real shim height (4mm) will lead to a better correspondence of the simulation data and the measurements near the shims.

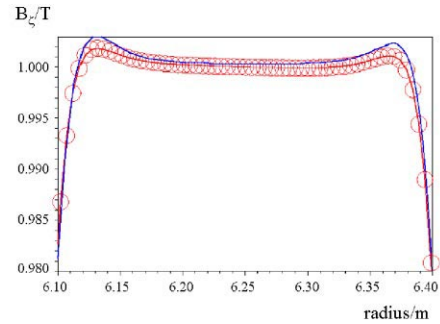


Figure 5: Simulated and measured magnetic flux density at the magnetic mid plane.

### 4.2 Optics of the Injection Line

We have integrated the reference trajectory for a particle rigidity of 6.234 Tm using the calculated field data (figure 6). The non-constant field expansion coefficients  $h(s)$  and  $k(s)$  are shown in figures 7 and 8. Further, the integrated principal trajectories are shown in figure 9 and the first order dispersion in 10. Finally table 5 summarizes the first order results for the combined transformation map  $M_1 M_s M_0$  including the drift spaces  $M_0$  and  $M_1$  as introduced in section 3. The entire path length calculated is 4.13 m.

## 5 CONCLUSION

The presented calculations give new insight into the real characteristics of the ESR injection line and serve for the

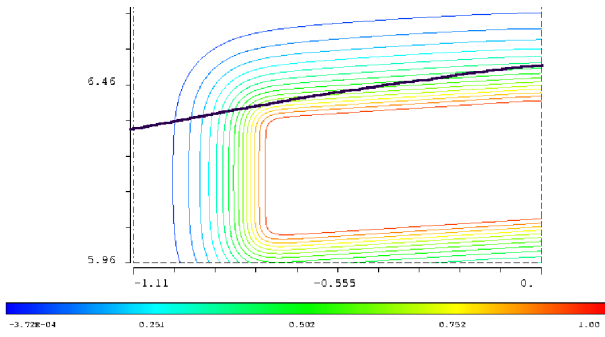


Figure 6: Magnetic flux density at the mid plane with calculated reference trajectory.

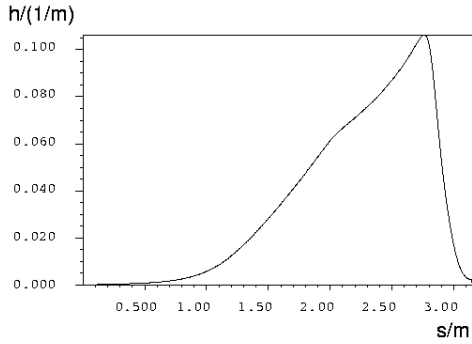


Figure 7: Parameter  $h(s)$  calculated for the ESR injection line.

definition of corrective measures. The calculated coefficients will be used in TRANSPORT and MAD simulations of the ESR.

## 6 REFERENCES

- [1] B. Franzke, et al., Commissioning of the Heavy Ion Storage Ring ESR, Proc. 2nd Europ. Part. Accel. Conf., Nice 1990, Vol.1, pp.46–48.
- [2] M. Chen, et al., Field Measurements of the ESR Magnets, Proc. 2nd Europ. Part. Accel. Conf., Nice 1990, Vol.2, pp.1142–1144.
- [3] B. Schillinger, T. Weiland, Beamtracking in Cylindrical and Cartesian Coordinates, CAP'96, to be published.
- [4] K. L. Brown, A First and Second Order Matrix Theory for the Design of Beam Transport Systems, SLAC 75, 1967.
- [5] K. G. Steffen, High Energy Beam Optics, Int. Publ., 1965.
- [6] B. Schillinger, T. Weiland, B. Langenbeck, Ion Injection through fringe fields of dipole magnets, Proc. 5th Europ. Part. Accel. Conf., Sitges(Barcelona) 1996, Vol.2, pp.1377–1379.
- [7] MAFIA Manual Version 4.00, CST GmbH, Lauteschlägerstr. 38, D–64289 Darmstadt, January 1997.

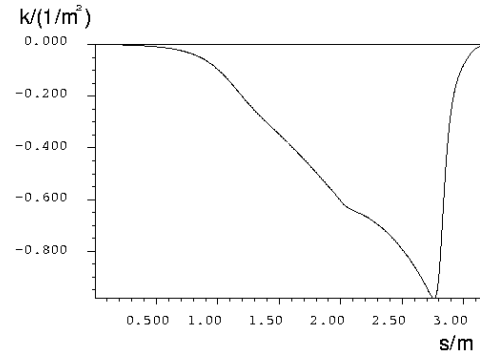


Figure 8: Parameter  $k(s)$  calculated for the ESR injection line.

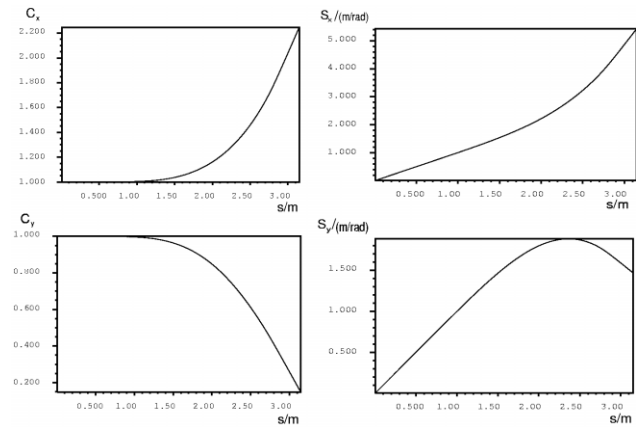


Figure 9: Principal trajectories of the ESR injection line.

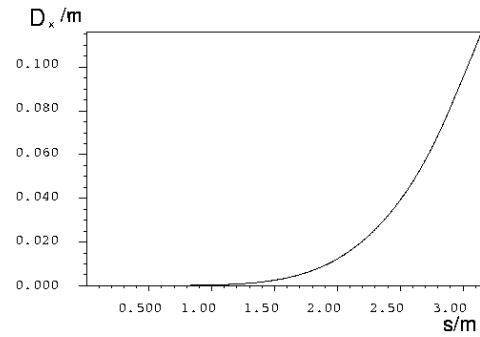


Figure 10: First order dispersion of the ESR injection line.

$(\mathbf{x}^1   \mathbf{x}^0)$	$x$	$x'$	$y$	$y'$	$l$	$\delta$
$x$	3.62	9.17	0	0	0	0.25
$x'$	1.40	3.82	0	0	0	0.14
$y$	0	0	-0.60	0.68	0	0
$y'$	0	0	-0.76	-0.80	0	0
$l$	0.15	0.32	0	0	1	3.6e-3
$\delta$	0	0	0	0	0	1

Table 1: Calculated first order coefficients of the combined transformation map.